ChemPubSoc Europe

DOI: 10.1002/chem.201502893

CHEMISTRY A European Journal Full Paper

Mesoporous Materials

Adsorptive Separation of Acetylene from Light Hydrocarbons by Mesoporous Iron Trimesate MIL-100(Fe)

Ji Woong Yoon,[a, b] Ji Sun Lee,[a, c] Sukyung Lee,[a] Kyoung Ho Cho,[a] Young Kyu Hwang,[a] Marco Daturi,[b] Chul-Ho Jun,[c] Rajamani Krishna,*[d] and Jong-San Chang*[a, e]

Abstract: A reducible metal–organic framework (MOF), iron(-III) trimesate, denoted as MIL-100(Fe), was investigated for the separation and purification of methane/ethane/ethylene/acetylene and an acetylene/CO_2 mixtures by using sorption isotherms, breakthrough experiments, ideal adsorbed solution theory (IAST) calculations, and IR spectroscopic analysis. The MIL-100(Fe) showed high adsorption selectivity not only for acetylene and ethylene over methane and ethane, but also for acetylene over CO_2. The separation and purification of acetylene over ethylene was also possible for MIL-100(Fe) activated at 423 K. According to the data obtained from operando IR spectroscopy, the unsaturated Fe^{III} sites and surface OH groups are mainly responsible for the successful separation of the acetylene/ethylene mixture, whereas the unsaturated Fe^{II} sites have a detrimental effect on both separation and purification. The potential of MIL-100(Fe) for the separation of a mixture of C_2H_2/CO_2 was also examined by using the IAST calculations and transient breakthrough simulations. Comparing the IAST selectivity calculations of C_2H_2/CO_2 for four MOFs selected from the literature, the selectivity with MIL-100(Fe) was higher than those of CuBTC, ZJU-60a, and PCP-33, but lower than that of HOF-3.

Introduction

It has been reported that the commercial separation of a mixture of hydrocarbons to give polymer-grade products requires an energy-intensive distillation process due to physicochemical similarities between the hydrocarbons.[1] Ethylene and acetylene, in particular, possess similar physicochemical characteristics and are important raw materials for the synthesis of various industrial and consumer products, such as acetic acid, rubber, and plastics.[2] Among the various efforts to replace the conventional distillation process to obtain polymer-grade raw materials, adsorptive separation appears to be one of the most promising short-term solutions.[3] However, for this process, effective adsorbents possessing high sorption capacities, high separation ratios, and facile regeneration properties have not yet been developed, despite a number of reports related to porous adsorbents, such as cationic zeolites.[4]

Metal–organic frameworks (MOFs) are currently of great interest and importance because they possess extremely high surface areas and pore volumes, well-ordered porous structures, a range of chemical functionalities, and can encompass a number of metal elements in their crystalline frameworks.[5–9] These properties enable their applications in gas purification and separation of gas mixtures.[10–13] One such porous MOF, namely, iron(III) trimesate $[\{Fe_3O(H_2O)_2F_{0.81}(OH)_{0.19}\}\{C_6H_3(CO_2)_3\}_2]\cdot n\,H_2O$ ($n \approx 14.5$), denoted as MIL-100(Fe), is based on μ_3-*oxo*-centered trimers of Fe^{III} octahedra.[14] As shown from IR spectroscopic studies on MIL-100(Fe),[15] the terminal water molecules can be removed from the framework by heating above 373 K either under vacuum or in a stream of gas, leading initially to a large number of coordinatively unsaturated sites (CUSs) for Fe^{III} acting as Lewis acids within the pores. The structural characteristics of MIL-100(Fe) indeed make it a good candidate for inducing reducibility on the framework iron sites; thus resulting in improvements in the preferential sorption properties of selected gas molecules. We recently reported the selective separation of propylene and propane on MIL-100(Fe) by using breakthrough and operando IR methodology.[15,16] We demonstrated that, with increasing the activation temperature of the sample, the separation effect increased due

[a] Dr. J. W. Yoon,[+] J. S. Lee,[+] S. Lee, K. H. Cho, Dr. Y. K. Hwang, Prof. Dr. J.-S. Chang
Research Center for Nanocatalysts
Korea Research Institute of Chemical Technology (KRICT)
P.O. Box 107, Yusung, Daejeon 305-600 (Korea)
E-mail: jschang@krict.re.kr

[b] Dr. J. W. Yoon,[+] Prof. Dr. M. Daturi
Laboratoire Catalyse et Spectrochimie
ENSICAEN, Université de Caen, CNRS
6 Bd. Maréchal Juin, 14050, Caen (France)

[c] J. S. Lee,[+] Prof. C.-H. Jun
Department of Chemistry, Center for Bioactive Molecular Hybrid
Yonsei University, Seodamoonku, Seoul 120-749 (Republic of Korea)

[d] Prof. Dr. R. Krishna
van 't Hoff Institute for Molecular Sciences
University of Amsterdam, Science Park 904
Amsterdam 1098 XH (The Netherlands)
E-mail: R.krishna@contact.uva.nl

[e] Prof. Dr. J.-S. Chang
Department of Chemistry, Sungkyunkwan University
Suwon 440-476 (Korea)

[+] These two authors contributed equally contributed to this work.

Supporting information for this article is available on the WWW under http://dx.doi.org/10.1002/chem.201502893.

to the reducible properties of MIL-100(Fe), that is, to an increased concentration of Fe^{II} sites. In fact, according to the operando approach,[16] the unsaturated Fe^{II} sites are mainly responsible for the separation effect of the C_3 mixture because of their affinity to unsaturated bonds, such as the C=C moiety in propylene.

In this work, we aim to explore the adsorptive separations of C_2 hydrocarbons, methane, and CO_2, in particular, the selective separation of acetylene over ethylene, by using MIL-100(Fe), through single-component adsorption isotherms and breakthrough experiments of hydrocarbon mixtures. Furthermore, operando IR spectroscopy is used to provide a better understanding of the interactions between MIL-100(Fe) and unsaturated C_2 hydrocarbons, such as acetylene and ethylene.

Results and Discussion

Single-component equilibrium adsorption isotherms of methane, ethane, ethylene, and acetylene on MIL-100(Fe) between 293 and 313 K after dehydration under vacuum at 425 K for 12 h are compared in Figure 1. The experimentally measured loadings for C_2H_2 and C_2H_4 in MIL-100(Fe) at temperatures of 293 and 313 K were also fitted with the dual-site Langmuir model (see the Supporting Information). The fitted parameter values for C_2H_2, C_2H_4, C_2H_6, and CH_4 are provided in Table S1 in the Supporting Information. The isotherm fits are excellent for all guest molecules over the entire pressure range at both temperatures. These isotherms exhibit a higher adsorption energy for C_2 hydrocarbons than methane under all pressures and temperatures studied, notably in the case of unsaturated C–C bonds. Ideal adsorbed solution theory (IAST) calculations of the component loadings for C_2H_2, C_2H_4, C_2H_6, and CH_4 for adsorption of a four-component equimolar mixture at 293 and 313 K show the following loading hierarchies at 100 kPa: $C_2H_2 > C_2H_4 > C_2H_6 > CH_4$ (Figure S1 in the Supporting Information).

The particularly high sorption affinities to ethylene and acetylene at low pressures (< 30 kPa) can be attributed to strong interactions between these molecules and the monolayer of specific sites on MIL-100(Fe).[15–17] Furthermore, MIL-100(Fe) was found to show a relatively large C_2H_2 uptake capacity (5.3 mmol g^{-1}) at 101 kPa and 293 K (Table 1). However, under similar conditions, this value is not comparable to the highest values reported for MOF materials.[12] Nevertheless, MIL-100(Fe) may still be considered a possible adsorbent for acetylene storage because it shows better hydrothermal and physicochemical properties than those of other MOF materials.[5] The sorption affinity for ethylene after dehydration under vacuum at 525 K increased up to 60% (Figure 1c), whereas the amount of acetylene adsorbed increased by only 25% (Figure 1d). Considering the results found for the separation of propane and propylene on MIL-100(Fe),[15,16] the higher sorption affinity for ethylene by MIL-100(Fe) activated at 525 K can be attributed to strong interactions between ethylene and the Fe^{II} CUSs.

To examine the interactions of C_2 hydrocarbons and methane with the MIL-100(Fe) adsorbent, the isosteric heats of adsorption as a function of adsorption loading were estimated by applying the Clausius–Clapeyron equation[18] to the respective adsorption isotherms recorded at two different temperatures.

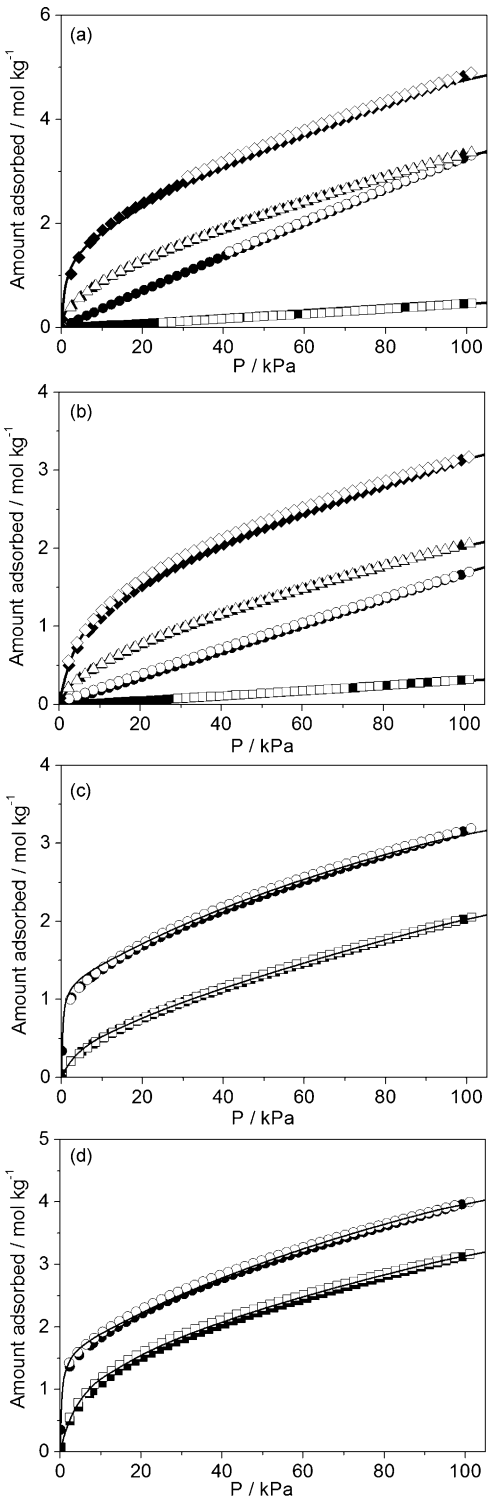

Figure 1. Single-component adsorption isotherms of methane (■□), ethane (●○), ethylene (▲△), and acetylene (◆◇) on MIL-100(Fe) at a) 293 and b) 313 K after dehydration at 425 K for 12 h. Comparison of adsorption isotherms of c) ethylene and d) acetylene at 313 K after dehydration at 425 K (■□) and 525 K (●○) for 12 h. The solid lines represent the dual-site Langmuir model isotherm.

Table 1. Comparison of acetylene uptakes in selected MOFs at 1 bar.

Materials[a]	BET surface area [$m^2 g^{-1}$]	C_2H_2 uptake [$cm^3 g^{-1}$]	T_{ad} [K]	Ref.
MIL-100(Fe)	2300	119	293	this work
$Cu_2(pzdc)_2(pyz)$	571	42	300	[12a]
$Fe_2(dobdc)$	1350	152	318	[12b]
NOTT-300	1370	142	293	[12c]
Mg(HCOO)	284	66	298	[12d]
Mn(HCOO)	297	51	298	[12d]
$Cu_2(PDDI)$	2823	193	298	[12e]
MOF-505	1694	148	298	[12f]
CuBTC (HKUST-1)	2095	201	295	[12f]
MIL-101(Cr)	4100	144	313	[12g]
$Zn_4L(DMA)_4$	660	97	296	[12h]
UTSA-100a	970	97	296	[12i]

[a] pzdc = pyrazine-2,3-dicarboxylate, pyz = pyrazine, H_4PDDI = 5,5′-(pyridine-2,5-diyl)diisophthalic acid, L = 1,2,4,5-tetra(5-isophthalic acid)benzene, DMA = *N*,*N*′-dimethylacetamide.

Figure 2 shows the isosteric heats of adsorption for four adsorbates. The isosteric heats of adsorption for methane and ethane were approximately −15 and −27 kJ mol^{-1}, respectively. No significant change was observed between loadings of 0 and 1.1 mmol g^{-1}. However, the isosteric heats of adsorption for ethylene (−61 kJ mol^{-1}) and acetylene (−65 kJ mol^{-1}) were significantly greater than those for methane and ethane at all adsorption loadings examined, which suggests a strong interaction between ethylene/acetylene and specific sites of the MOF framework. However, it was found to decrease gradually with increasing adsorption loading, which indicated the energetic heterogeneity of the adsorbent surface.

On the basis of the component loadings of the sample activated at 423 K (Figure S1 A in the Supporting Information), we also calculated the selectivities of separation, S_{ads}, of the four constituent binary pairs: C_2H_2/C_2H_4, C_2H_2/C_2H_6, C_2H_4/C_2H_6, and C_2H_6/CH_4 (Figure 3). Except for the C_2H_4/C_2H_6 pair, the other three selectivities at a total pressure of 100 kPa were higher than about three, which indicated that each of the four components could be recovered in nearly pure form from four-component mixtures.

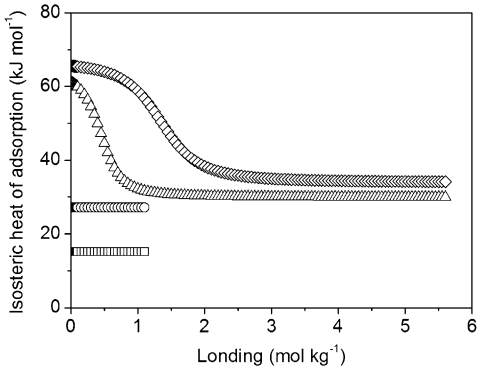

Figure 2. Isosteric heats of adsorption ($-\Delta H_{ads}$) for methane (□), ethane (○), ethylene (△), and acetylene (◇) on MIL-100(Fe) based on adsorption loadings between 0 and 6 mmol g^{-1}. The sample was activated at 425 K for 12 h before adsorption was measured.

The separations of binary and ternary mixtures were investigated in terms of breakthrough column experiments to confirm the separation performance of the MIL-100(Fe) adsorbent. The sample was first activated in a flow of argon at 373–523 K for 12 h to determine the relative contribution of surface sites in the separation. Figure 4 shows the breakthrough curves of binary equimolar mixtures of C_2H_6/C_2H_4, C_2H_6/C_2H_2, and C_2H_4/C_2H_2 with a partial pressure of 5 kPa in argon at 313 K. Although an increase in the activation temperature increased the amount of ethylene and acetylene adsorbed onto MIL-100(Fe) used for paraffin/olefin separation, a similar amount of ethane was adsorbed at each activation temperature (Figure 4 a and b). From these curves, the separation factors, α, for ethylene and acetylene over ethane were estimated to be 17 and 21 for the sample activated at 523 K, and 5 and 7 for that treated at 373 K, respectively. This result clearly demonstrates that separation of C_2 hydrocarbons at low pressures is greatly improved in the presence of F^{II} CUS, although a small number of Fe^{III}

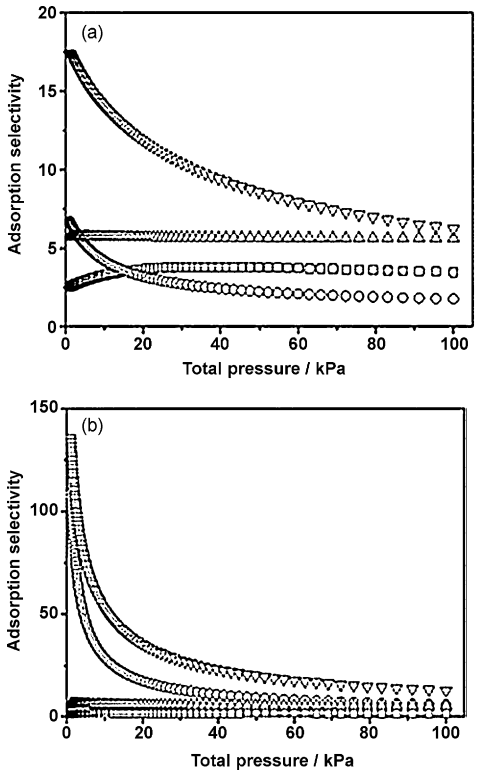

Figure 3. IAST calculations of adsorption selectivities of C_2H_2/C_2H_4 (□), C_2H_4/C_2H_6 (○), C_2H_6/CH_4 (△) and C_2H_2/C_2H_6 (▽) at 313 K. The sample was activated for 12 h at a) 423 and b) 523 K.

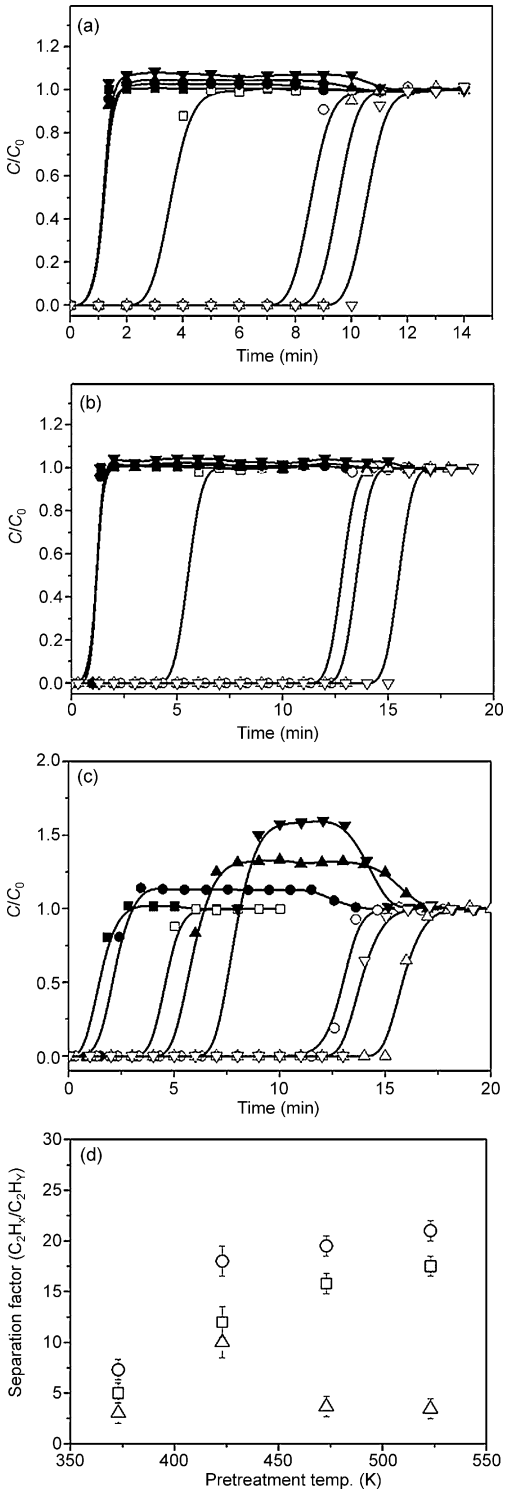

Figure 4. Breakthrough curves of equimolar mixtures of a) C_2H_6 (filled symbols) and C_2H_4 (open symbols), b) C_2H_6 (filled symbols) and C_2H_2 (open symbols), and c) C_2H_4 (filled symbols) and C_2H_2 (open symbols) in argon ($p = 5$ kPa) on MIL-100(Fe) at 313 K after activation at 373 (■□), 425 (●○), 473 (▲△), and 525 K (▼▽). d) Separation factor, α, for $C_{ethylene}/C_{ethane}$ (□), $C_{acetylene}/C_{ethane}$ (○), and $C_{acetylene}/C_{ethylene}$ (△) obtained from breakthrough curves of MIL-100(Fe) at a partial pressure of $p = 5$ kPa.

CUS sites are also associated with ethylene and acetylene adsorption. On the contrary, an increase in the activation temperature had no effect on the separation factors for C_2H_4/C_2H_2, which both have unsaturated C–C bonds. The highest separation factor for C_2H_4/C_2H_2 was about 10 after dehydration at 423 K; however, the separation factors for C_2H_4/C_2H_2 were generally below 4 at all other temperatures (Figure 4d). With regard to C_3 separation on MIL-100(Fe),[15,16] the adsorption of ethylene and acetylene over ethane mixtures (for paraffin/olefin) increase markedly with an increase in the activation temperature. In the separation of C_2H_4/C_2H_2 (Figure 4c), the amount of ethylene adsorption increased when the activation temperature increased from 373 to 523 K, although acetylene adsorption from the gas mixture increased up to an activation temperature of 473 K. In addition, at an activation temperature of 523 K, the amount of acetylene adsorbed relative to the amount of ethylene adsorbed was lower than those at lower activation temperatures.

To understand the unexpected effect of the activation temperature on the separations of C_2 hydrocarbons, we performed IR spectroscopic measurements on MIL-100(Fe) under flow conditions by using the operando methodology. In the gas phase, acetylene presents only two IR-active bands, the νasym(≡C–H) stretch at $\tilde{\nu} = 3284\ cm^{-1}$ and the δasym(≡C–H) bend at $\tilde{\nu} = 613\ cm^{-1}$, which are red- and blueshifted, respectively, upon adsorption of the molecule on a solid surface. In such a case, also a third vibration, the ν(C≡C) stretch at $\tilde{\nu} = 1974\ cm^{-1}$, becomes active and redshifted.[20] The distortion of the molecule subsequent to adsorption activates the ν_{sym}(≡C–H) stretch at $\tilde{\nu} = 3374\ cm^{-1}$ (red-shifted) and the δ_{sym}(≡C–H) bend at $\tilde{\nu} = 730\ cm^{-1}$ (blue-shifted) as well, whereas the appearance of additional components can be because the C–H bonds in acetylene are no longer equivalent upon adsorption,[21] which makes the interpretation of spectra quite complicated. The interaction modes can be end-on and parallel, as determined by strong polarization of the π bonds.[22] Alternatively, the molecule can interact by hydrogen bonding with basic sites or undertake a dissociative adsorption on neighboring acid–base pairs. The two last adsorption modes can be discarded in the present case, as already established after propyne adsorption in a previous study.[23] To help spectral interpretation, an in situ study has been performed, by introducing a flow of acetylene onto the sample at different partial pressures and after material activation at 373, 423, 473, and 523 K (Figure S2 in the Supporting Information). For the sake of clarity, the region of OH stretches has also been reported versus the activation temperature (Figure S3 in the Supporting Information); we observe two bands at $\tilde{\nu} = 3680$ and $3607\ cm^{-1}$ due to molecular water coordinatively adsorbed on Fe^{III} CUS,[23] a band at $\tilde{\nu} = 3700\ cm^{-1}$ associated with Fe^{III} hydroxyls, and a component at $\tilde{\nu} = 3618\ cm^{-1}$ that can be assigned to OH groups on Fe^{II}.[24] After activation at 373 K (Figure S2a and S3 in the Supporting Information), molecular water coordinatively adsorbed on Fe^{III} CUS persists; the corresponding bands at $\tilde{\nu} = 3680$ and $3607\ cm^{-1}$ are perturbed (negative bands) by acetylene, adsorbed on the corresponding surface. At the same time, a hydroxyl group near $\tilde{\nu} = 3700\ cm^{-1}$ is shifted downward, which suggests hydrogen bonding with the acetylene molecules. Considering the reciprocal variation in intensity of

the bands, it seems that this interaction of OH groups is correlated with the band at $\tilde{\nu}=3158\ cm^{-1}$. After treatment at 423 K, dehydroxylation increases, so that the bands corresponding to acetylene adsorption also increase in intensity, especially that at $\tilde{\nu}=3222\ cm^{-1}$, which is likely to be related to Fe^{III} CUS, whereas that assigned to the interaction with OH groups shifts to $\tilde{\nu}=3172\ cm^{-1}$.[25] Other features appear at higher wavenumber, notably a sharp component that increases in intensity after thermal treatment at 473 K. This band at $\tilde{\nu}=3256\ cm^{-1}$ grows with thermal treatment (Figure S2 c and d in the Supporting Information), as the Fe^{II} sites clearly appear and increase in concentration; therefore, this band could be assigned to acetylene coordination on the Fe^{II} CUS. This assignment is also supported by the results of Bordiga et al.,[20] who found a band at $\tilde{\nu}=3244\ cm^{-1}$ upon acetylene adsorption on CPO-27(Fe), in which only Fe^{II} existed.

Figure 5 shows the behavior of the sample in contact with ethylene or acetylene gas diluted in argon. As can be seen in Figure 5 a, for MIL-100(Fe) activated at 373–523 K for 12 h, the IR spectra clearly show bands corresponding to adsorbed acetylene, as discussed above. The different assignments are summarized in Table 2. These results indicate that Fe^{III} and Fe^{III}–OH sites are mainly responsible for the adsorption of acetylene on MIL-100(Fe) activated at 423 K. Clearly, the peaks related to Fe^{III}–OH sites disappeared when activation was carried out above 473 K for 12 h, whereas the peaks corresponding to acetylene coordinated on Fe^{III} ($\tilde{\nu}=3222\ cm^{-1}$) and Fe^{II} ($\tilde{\nu}=3242\ cm^{-1}$) sites increased (Figure S4 in the Supporting Information). We also observed a decrease in the intensity of the coordinated water and OH groups at $\tilde{\nu}=3607$ and 3704 cm^{-1} and an increase in the band intensities at $\tilde{\nu}=3458$ and 3677 cm^{-1} due to the formation of hydrogen bonds with acetylene. These bands disappeared when acetylene gas in the flux was switched off. We could therefore conclude that the interaction of acetylene with the OH groups of MIL-100(Fe) was rather weak. From the results of Gaussian multipeak fitting for IR spectra in the $\tilde{\nu}=3100$–$3300\ cm^{-1}$ range (Figure S4 in the Supporting Information), the peak areas at $\tilde{\nu}=3160$–$3180\ cm^{-1}$, corresponding to the interaction of the OH groups with acetylene, decreased at higher activation temperatures. In contrast, an increase in the band at $\tilde{\nu}=3320$–$3330\ cm^{-1}$, corresponding to the Fe^{III} sites, and at $\tilde{\nu}=3342\ cm^{-1}$, corresponding to the Fe^{II} sites, was observed with increasing activation temperature. The characterization of ethylene adsorption is more complex, due to the superimposition of the characteristic bands of the molecule on the carboxylate motifs of the solid. However, the olefin should undertake π coordination with the surface sites, and have a limited interaction with OH groups.[22] Figure 5 b shows the IR spectra of the region corresponding to the ethylene adsorption vibration[26] on MIL-100(Fe) activated at 373–523 K for 12 h. We would like to comment on two bands, in particular: at $\tilde{\nu}=982$ and 987 cm^{-1}; the latter appears after activation at 473 K and grows in intensity after thermal treatment at higher temperature. Therefore, we can tentatively assign it to ethylene adsorbed on Fe^{II} sites. The other band at $\tilde{\nu}=982\ cm^{-1}$, which is present after activation at lower temperature, exhibits a very low intensity with activation temperatures above 473 K due to very weak interactions of ethylene with the Fe^{III} sites. Moreover, an increase in the intensity of the band at $\tilde{\nu}=987\ cm^{-1}$ with increasing activation temperature, as observed for acetylene adsorption, supports the hypothesis that ethylene mainly interacts with the Fe^{II} sites in MIL-100(Fe). However, an additional understanding is required with regard to interactions with acetylene, which can be achieved through the characterization of the thermal behavior under flow conditions.

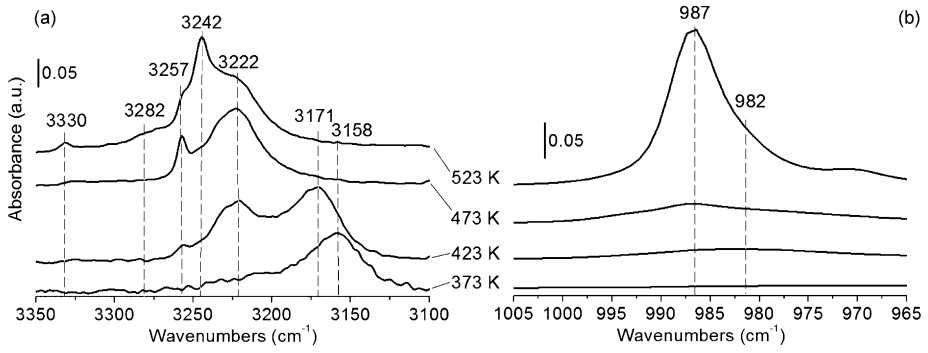

Figure 5. FTIR spectra of MIL-100(Fe) exposed to gas streams containing a) 1000 ppm acetylene and b) 1000 ppm ethylene at 313 K after activation under an argon flow at a range of temperatures for 12 h.

Table 2. Frequencies of C_2H_2 vibrational modes in the gas phase and adsorbed on MIL-100(Fe) and CPO-27(Fe).

Material		Vibrational frequencies [cm^{-1}]				Ref.
		ν_{asym}(C–H)	δ_{sym} (C–H)	ν_{sym}(C–H)	ν_{sym} (C≡C)	
gas phase		3284	730	3374	1974	[18]
CPO-27(Fe)		3244	734, 755	3300	1937	[19]
MIL-100(Fe)	Fe^{II}	3245, 3282	772	3330	1954	this work and ref. [21]
	Fe^{III}	3222, 3256	–	–		
	OH or H	3158, 3172	–	–	–	

As we demonstrated for C_3 separation on MIL-100(Fe),[16] it is possible to use NO to selectively block the Fe^{II} CUSs. It is also possible to poison one of the two possible adsorption sites (Fe^{II} or Fe^{III}) and to subsequently investigate the sorption affinity to unsaturated C_2 hydrocarbon mixtures (ethylene/acetylene). Figure 6 shows the breakthrough curves of an equimolar mixture of C_2H_4/C_2H_2 ($p=5$ kPa) at 313 K, both with and without NO saturation on the activated MIL-100(Fe) (Ar flow at 423 and 523 K for 12 h). The adsorption of ethylene and acetylene dramatically decreased after blocking the Fe^{II} sites with NO. This demonstrates that the Fe^{II} sites show selective sorption toward

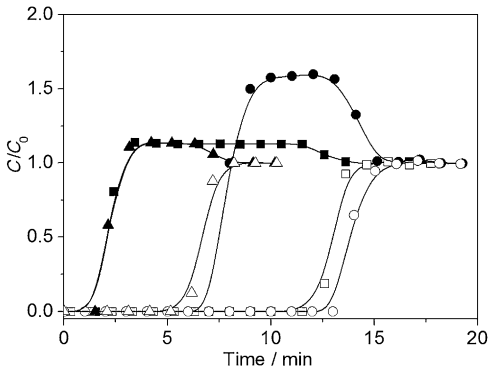

Figure 6. Breakthrough curves in the separation of an equimolar mixture of C_2H_4 (filled symbols) and C_2H_2 (open symbols) in argon ($p = 5$ kPa) on MIL-100(Fe) at 313 K: ■□: sample activated at 423 K for 12 h, ●○: sample activated at 523 K for 12 h, ▲△: sample activated at 523 K followed by NO adsorption at 313 K to block Fe^{II} sites.

NO over the olefin mixture. Because the CUSs have been confirmed in dehydrated MIL-100(Fe) by CO adsorption,[15] the appearance of the Fe^{II} CUS was observed above 473 K. It appears that the adsorptive separation of a mixture of C_2H_2/C_2H_4 is negatively affected by the presence of Fe^{II} sites on MIL-100(Fe); this is likely to be because of a strong, unselective adsorption of both molecules on these sites. As illustrated in Figure 7, the IR spectra showed the presence of bands at $\tilde{\nu} = 3100$–$3400\ cm^{-1}$, which correspond to interactions between acetylene and the Fe^{III}, Fe^{II}, and Fe^{III}–OH sites, as mentioned previously. Among these bands, the ν_{asym}(CH) mode at $\tilde{\nu} = 3244\ cm^{-1}$, corresponding to the interaction of acetylene with the Fe^{II} sites, disappeared after NO saturation of MIL-100(Fe) under activation at 523 K for 12 h. This indicates that acetylene interactions with Fe^{III} sites on MIL-100(Fe) are solely observed after NO saturation.

To evaluate the separation efficiency for the mixture of ethane/ethylene/acetylene, breakthrough tests of the ternary mixture in argon ($P(C_2H_6) = 2.5$ kPa, $P(C_2H_4) = 2.5$ kPa, and $P(C_2H_2) = 2.5$ kPa) were performed on MIL-100(Fe). The sample was activated in a flow of argon at both 423 and 525 K for 12 h to determine the relative contribution of the Fe^{II}, Fe^{III}, and OH sites in the separation. As in the separation of the binary mixture, the separation factor of the C_2H_2/C_2H_4 mixture on MIL-100(Fe) activated at 423 K was higher than the separation efficiency at higher activation temperatures. However, the separation efficiency for the mixture of C_2H_4/C_2H_6 exhibited the opposite effect, due to the preferential coordination of the olefin with the Fe^{II} sites. To effectively separate the ternary mixture of $C_2H_6/C_2H_4/C_2H_2$ (Figure S6 in the Supporting Information) and quaternary mixture of $CH_4/C_2H_6/C_2H_4/C_2H_2$ (Figure 8), a two-step separation process could be proposed, which consisted of acetylene separation with MIL-100(Fe) activated at 423 K, followed by ethylene separation from ethane with MIL-100(Fe) activated at 523 K. Therefore, sorption and IR analysis results shown above suggest that the surface properties of MIL-100(Fe) in terms of OH and $Fe^{II/III}$ CUSs would lead to good separation efficiency for C_2 mixtures under tailored activation conditions. This result highlights the importance of the surface properties of MOFs in their applications as adsorbents for selective sorption processes.

The separation of a mixture of C_2H_2/CO_2 is important in industry for the production of pure C_2H_2, which is required for a variety of applications in the petrochemical and electronic industries.[27] This separation is difficult because of the similarity in molecular dimensions and molecular properties.[27–29] However, MIL-100(Fe) has the potential for the separation of mixtures of C_2H_2/CO_2 as the separation of C_2 hydrocarbons. The experimentally measured isotherm for CO_2 at temperatures of 303 K was fitted with the single-site Langmuir model. The isotherm data for C_2H_2 used in the selectivity calculations were for MIL-100(Fe) activated at 423 K. Figure 9 compares the IAST calculations of adsorption selectivity, S_{ads}, for the separation of a 50/50 mixture of C_2H_2/CO_2 for MIL-100(Fe) at 303 K with that of four other MOFs known to selectively adsorb C_2H_2: HOF-3,[30] CuBTC,[30] ZJU-60a,[31] and PCP-33.[32] The IAST selectivity calculations for these four MOFs, available at 296 K, were taken from published results.[29] Notably, the selectivity with MIL-100(Fe) is higher than those of CuBTC, ZJU-60a, and PCP-33, but lower than that of HOF-3. As mentioned above, after activation at 423 K, the unsaturated Fe^{III} sites and surface hydroxyl groups are mainly responsible for the high sorption affinity to acetylene. The mesoporosity of MIL-100(Fe) induces lower CO_2 uptakes than those of microporous MOFs, such as CuBTC, at low pressure below 101 kPa. The combined

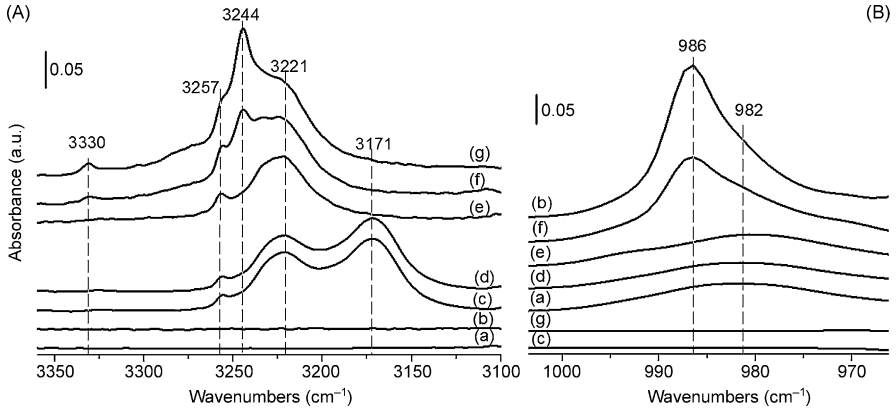

Figure 7. FTIR spectra of MIL-100(Fe) upon saturation for A) acetylene and B) ethylene adsorption, depending on activation temperature and NO preadsorption treatment bands on MIL-100(Fe) activated at 423 and 523 K for 12 h with and without NO saturation: a) ethylene adsorption after activation at 423 K for 12 h, b) ethylene adsorption after activation at 523 K for 12 h, c) acetylene adsorption after activation at 423 K for 12 h, d) ethylene and acetylene adsorption after activation at 423 K for 12 h, e) ethylene and acetylene adsorption after activation at 523 K for 12 h followed by NO saturation at 298 K, f) ethylene and acetylene adsorption after activation at 523 K for 12 h, and g) acetylene adsorption after activation at 523 K for 12 h.

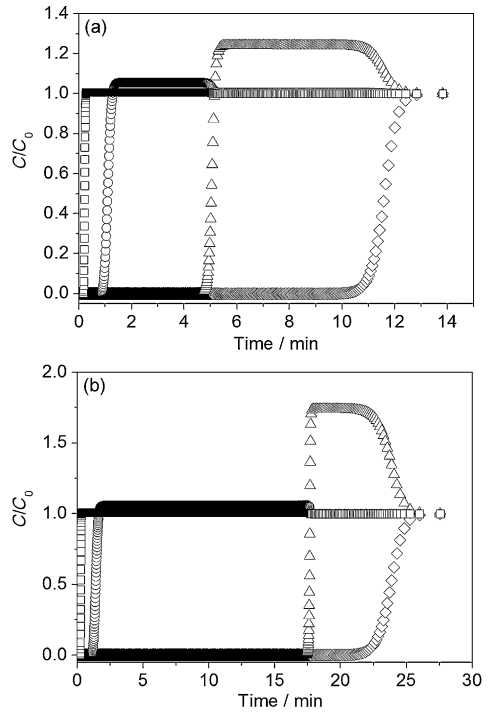

Figure 8. Transient breakthrough simulations for equimolar CH_4 (□), C_2H_6 (○), C_2H_4 (△), and C_2H_2 (◇) in argon at 313 K on MIL-100(Fe) activated for 12 h at a) 423 and b) 523 K. The partial pressures of each hydrocarbon in the entering gas mixture was 2.5 kPa. The total pressure was 101 kPa.

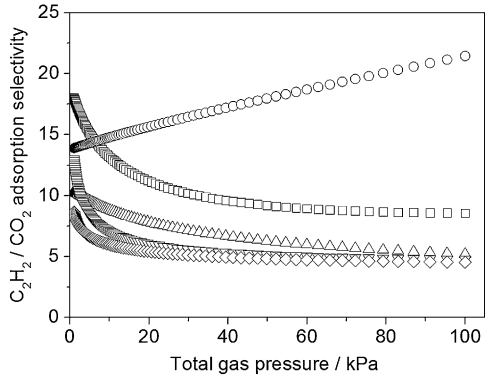

Figure 9. IAST calculations of adsorption selectivity, S_{ads}, for the separation of 50/50 mixtures of C_2H_2/CO_2 with MIL-100(Fe) (□), HOF-3 (○),[30] CuBTC (△),[30] ZJU-60a (▽),[31] and PCP-33 (◇).[32]

sorption properties of MIL-100(Fe) exhibit a relatively good selectivity for the separation of acetylene over CO_2. The transient breakthrough of separations of a mixture of C_2H_2/CO_2 also demonstrates the separation potential of MIL-100(Fe) (Figure S7 in the Supporting Information).

Conclusion

The gas-selective sorption properties of MIL-100(Fe) showed that this material displayed high selectivity not only for ethylene and acetylene over ethane and methane, but also for acetylene over CO_2, in addition to a high preferential selectivity for acetylene over ethylene, depending on the activation conditions employed. Operando IR spectra of MIL-100(Fe) confirmed strong interactions between the Fe^{III} CUS and surface OH sites with acetylene, but only a weak interaction with ethylene. These properties led to a high separation factor for acetylene over ethylene in both binary and ternary gas mixtures. However, when the Fe^{II} CUS was present, a lower separation factor for acetylene over ethylene was observed due to the nonselective adsorption of acetylene and ethylene at the Fe^{II} sites, in other words, the strong adsorption of both gases at the Fe^{II} sites. On the contrary, this characteristic is positive in the presence of molecules with saturated C–C bonds because the absence of multiple bonds prevent π interactions of the molecules with the surface; therefore, promoting a high separation between alkanes and olefins. These sorption data suggest the potential for the adsorptive separation of C_1/C_2 hydrocarbons and CO_2 mixtures with MIL-100(Fe), depending on the activation temperature.

Experimental Section

Sample preparation and characterization: According to a synthesis protocol previously reported elsewhere,[15] MIL-100(Fe) was prepared from a hydrothermal reaction of 1,3,5-benzenetricarboxylic acid (1,3,5-BTC) with metallic iron, HF, nitric acid, and H_2O. The composition of the reaction mixture was 1.0 Fe/0.67 1,3,5-BTC/2.0 HF/0.6 HNO_3/277 H_2O. The reaction mixture was loaded into a Teflon autoclave, heated to 423 K, and held at this temperature for 12 h. The reaction mixture remained acidic throughout the preparation. After 12 h, the resulting light-orange solid was recovered by filtration, and washed with deionized water. The resulting MIL-100(Fe) was purified further through a two-step process with hot water and ethanol. First, MIL-100(Fe) (1 g) was treated with boiling water (350 mL) at 353 K for 5 h to decrease the amount of residual unreacted ions. The MIL-100(Fe) was then treated with boiling ethanol at 333 K for 3 h until no colored impurities were detected in the mother liquor solution to give the highly purified MIL-100(Fe). Finally, the resulting solid was dried overnight below 373 K under a nitrogen atmosphere.

Sorption experiments: The sorption experiments were conducted by using a Micromeritics Tristar 3020 system, with methane (99.9999%), ethane (99.95%), ethylene (99.95%), acetylene (99.9%), and CO_2 (99.9%) (all obtained from Rigas corp.) at either 293 or 313 K (heated on a water bath) after dehydration under vacuum at 423 and 523 K for 12 h.

Breakthrough experiments: Transient breakthrough curves were then obtained by using a fixed-bed flow system apparatus equipped with a stainless-steel column (4.15 mm inner diameter × 80 mm height) under atmospheric pressure. Before carrying out the breakthrough experiments, the MIL-100(Fe) powder was pelletized ($< 50\ kg_f cm^{-2}$), crushed, and sieved to obtain particles of 0.3–0.5 mm in size. After pelletization, the sample (0.5 g) was activated at 373–523 K with argon (15 mL min^{-1} standard temperature and pressure (STP)). Gas mixtures of methane (2.5 kPa), ethane (2.5 kPa), ethylene (2.5 kPa), and acetylene (2.5 kPa) in argon (15 mL min^{-1} STP) were used for the experiments. The outlet gases of the breakthrough column were analyzed inline by using a gas chromatograph equipped with a flame ionization detector (FID).

Operando IR spectroscopic measurements: IR measurements for the determination of ethylene and acetylene adsorption were performed at 313 K after dehydration under argon (15 mL min^{-1}) at 373–523 K for 12 h in a "sandwich" reactor cell.[16] A reaction gas composed of ethylene (1000 ppm) and acetylene (up to 1500 ppm) in argon (15 mL min^{-1}) was used for the adsorption experiments. A gas mixture of ethylene (5000 ppm) and acetylene (1000 ppm) in argon (15 mL min^{-1}) was used for the experiments. A mixture of NO (5000 ppm) in argon (15 mL) was used for the saturation of Fe^{II} CUSs on MIL-100(Fe). After the NO concentration returned to its original level, the system was switched to the reaction flow for 30 min. The ethylene/acetylene mixture was then passed through the sample.

Acknowledgements

We would like to acknowledge financial support from the DRC Program (SK-1411) and the R&D Convergence Program (CRC-14-1-KRICT) of MSIP (Ministry of Science, ICT and Future Planning) and NST (National Research Council of Science & Technology) of the Republic of Korea. M.D. acknowledges financial support from an international collaboration program of KRICT (KK-1507M03). J.W.Y. acknowledges a post-doctoral fellowship supported by the Basic Science Research Program, through the National Research Foundation of Korea (NRF), funded by the Ministry of Education (2012R1A6A3A03040053).

Keywords: adsorption · gas separation · iron · IR spectroscopy · metal–organic frameworks

[1] R. B. Eldridge, *Ind. Eng. Chem. Res.* **1993**, *32*, 2208 – 2212.
[2] a) R. W. Baker, *Ind. Eng. Chem. Res.* **2002**, *41*, 1393 – 1411; b) Ullmann's Encyclopedia of Industrial Chemistry, 6th ed. (Ed.: B. Elvers), Wiley-VCH, Weinheim, **2001**.
[3] R. Kumar, T. C. Golden, T. R. White, A. Rokicki, *Sep. Tech.* **1992**, *27*, 2157 – 2170.
[4] a) D. L. Peterson, F. Helfferich, R. K. Griep, in: *Molecular Sieves* p 217 – 229 Proc. 1st Int. Conf. On Molecular Sieves, London **1967** published by Soc. for Chem. Ind. in **1968**; b) E. R. Gilliland, H. L. Bliss, C. E. Kip, *J. Am. Chem. Soc.* **1941**, *63*, 2088 – 2090.
[5] a) G. Férey, *Chem. Soc. Rev.* **2008**, *37*, 191 – 214; b) G. Férey, C. Mellot-Draznieks, C. Serre, F. Millange, J. Dutour, S. Surblé, I. Margiolaki, *Science* **2005**, *309*, 2040 – 2042; c) Y. K. Hwang, D.-Y. Hong, J.-S. Chang, S. H. Jhung, Y.-K. Seo, J. Kim, A. Vimont, M. Daturi, C. Serre, G. Férey, *Angew. Chem. Int. Ed.* **2008**, *47*, 4144 – 4148.
[6] a) O. M. Yaghi, M. O'Keeffe, N. W. Ockwig, H. K. Chae, M. Eddaoudi, J. Kim, *Nature* **2003**, *423*, 705 – 714.
[7] a) S.-I. Noro, S. Kitagawa, M. Kondo, K. Seki, *Angew. Chem. Int. Ed.* **2000**, *39*, 2081 – 2084; *Angew. Chem.* **2000**, *112*, 2161 – 2164; b) R. Kitaura, S. Kitagawa, Y. Kubota, T. C. Kobayashi, K. Kindo, Y. Mita, A. Matsuo, M. Kobayashi, H.-C. Chang, T. C. Ozawa, M. Suzuki, M. Sakata, M. Takata, *Science* **2002**, *298*, 2358 – 2361; c) S. Kitagawa, R. Kitaura, S.-I. Noro, *Angew. Chem. Int. Ed.* **2004**, *43*, 2334 – 2375; *Angew. Chem.* **2004**, *116*, 2388 – 2430.
[8] X. Zhao, B. Xiao, A. J. Fletcher, K. M. Thomas, D. Bradshaw, M. J. Rosseinsky, *Science* **2004**, *306*, 1012 – 1015.
[9] S. Chui, S. Lo, J. Charmant, A. Orpen, I. D. Williams, *Science* **1999**, *283*, 1148 – 1150.
[10] a) M. Eddaoudi, J. Kim, N. Rosi, D. Vodak, J. Wachter, M. O'Keeffe, O. M. Yaghi, *Science* **2002**, *295*, 469 – 472; b) J. L. C. Rowsell, O. M. Yaghi, *Angew. Chem. Int. Ed.* **2005**, *44*, 4670 – 4679; *Angew. Chem.* **2005**, *117*, 4748 – 4758; c) D. J. Collins, H. C. Zhou, *J. Mater. Chem.* **2007**, *17*, 3154 – 3160; d) L. J. Murray, M. Dinca, J. R. Long, *Chem. Soc. Rev.* **2009**, *38*, 1294 – 1314; e) J. Canivet, A. Fateeva, Y. Guo, B. Coasne, D. Farrusseng, *Chem. Soc. Rev.* **2014**, *43*, 5594 – 5617.
[11] a) R. Kitaura, K. Seki, G. Akiyama, S. Kitagawa, *Angew. Chem. Int. Ed.* **2003**, *42*, 428 – 431; *Angew. Chem.* **2003**, *115*, 444 – 447; b) J. Won, J. S. Seo, J. H. Kim, H. S. Kim, Y. S. Kang, S.-J. Kim, Y. Kim, J. Jegal, *Adv. Mater.* **2005**, *17*, 80 – 84.
[12] a) E. D. Bloch, W. L. Queen, R. Krishna, J. M. Zadrozny, G. M. Brown, J. R. Long, *Science* **2012**, *335*, 1606 – 1610; b) S. Yang, A. J. Ramirez-Cuesta, R. Newby, V. Garcia-Sakai, P. Manuel, S. K. Callear, S. I. Campbell, C. C. Tang, M. Schroder, *Nat. Chem.* **2014**, *7*, 121 – 129; c) D. G. Samsonenko, H. Kim, Y. Sun, G.-H. Kim, H.-S. Lee, K. Kim, *Chem. Asian J.* **2007**, *2*, 484 – 488; d) X. Rao, J. Cai, J. Yu, Y. He, C. Wu, W. Zhou, T. Yildirim, B. Chen, G. Qian, *Chem. Commun.* **2013**, *49*, 6719 – 6721; e) S. Xiang, W. Zhou, J. M. Gallegos, Y. Liu, B. Chen, *J. Am. Chem. Soc.* **2009**, *131*, 12415 – 12419; f) S.-J. Lee, J. W. Yoon, Y.-K. Seo, M.-B. Kim, S.-K. Lee, U.-H. Lee, Y. K. Hwang, Y.-S. Bae, J.-S. Chang, *Microporous Mesoporous Mater.* **2014**, *193*, 160 – 165; g) Y. He, Z. Zhang, S. Xiang, F. R. Fronczek, R. Krishna, B. Chen, *Chem. Eur. J.* **2012**, *18*, 613 – 619; h) T.-H. Hu, H. Wang, B. Li, R. Krishna, H. Wu, W. Zhou, Y. Zhao, Y. Han, X. Wang, W. Zhu, Z. Yao, S. Xiang, B. Chen, *Nat. Commun.* **2015**, *6*, 7328.
[13] J. W. Yoon, S. H. Jhung, Y. K. Hwang, M. Humphrey, P. T. Wood, J.-S. Chang, *Adv. Mater.* **2007**, *19*, 1830 – 1834.
[14] P. Horcajada, S. Surbl, C. Serre, D.-Y. Hong, Y.-K. Seo, J.-S. Chang, J.-M. Greneche, I. Margiolaki, G. Ferey, *Chem. Commun.* **2007**, 2820 – 2822.
[15] J. W. Yoon, Y.-K. Seo, Y. K. Hwang, J.-S. Chang, H. Leclerc, S. Wuttke, P. Bazin, A. Vimont, M. Daturi, E. Bloch, P. L. Llewellyn, C. Serre, P. Horcajada, J.-M. Greneche, A. E. Rodrigues, G. Ferey, *Angew. Chem. Int. Ed.* **2010**, *49*, 5949 – 5952; *Angew. Chem.* **2010**, *122*, 6085 – 6088.
[16] S. Wuttke, P. Bazin, A. Vimon, C. Serre, Y.-K. Seo, Y. K. Hwang, J.-S. Chang, G. Ferey, M. Datrui, *Chem. Eur. J.* **2012**, *18*, 11959 – 11967.
[17] a) T. Lesage, C. Verrier, P. Bazin, J. Saussey, M. Daturi, *Phys. Chem. Chem. Phys.* **2003**, *5*, 4435 – 4440; b) I. Malpartida, E. Ivanova, M. Mihaylov, K. Hadjiivanov, V. Blasin-Aube, O. Marie, M. Daturi, *Catal. Today* **2010**, *149*, 295 – 303.
[18] J. M. Thomas, W. J. Thomas, *Introduction to the Principles of Heterogeneous Catalysis*, Academic Press, New York, **1967**, p. 102.
[19] G. Herzberg, Molecular Spectra and Molecular Structure II. Infrared and Raman Spectra of Polyatomic Molecules, 7th ed., D. Van Nostrand, Princeton, **1956**.
[20] S. M. Chavan, G. C. Shearer, E. Bloch, S. Bordiga, *ChemPhysChem* **2012**, *13*, 445 – 448.
[21] S. Huber, H. Knözinger, *J. Mol. Catal. A* **1999**, *141*, 117 – 127.
[22] A. Davydov, Molecular spectroscopy of oxide catalyst surfaces (Ed.: N. T. Sheppard), Wiley, Chichester (UK), **2003**.
[23] H. Leclerc, A. Vimont, J.-C. Lavalley, M. Daturi, A. D. Wiersum, P. L. Llwellyn, P. Horcajada, G. Férey, C. Serre, *Phys. Chem. Chem. Phys.* **2011**, *13*, 11748 – 11756.
[24] C. Rémazeilles, Ph. Refait, *Polyhedron* **2009**, *28*, 749 – 756.
[25] A. V. Ivanov, A. e. Koklin, E. B. Uvarova, L. M. Kustov, *Phys. Chem. Chem. Phys.* **2003**, *5*, 4718 – 4723.
[26] G. Busca, V. Lorenzelli, G. Ramis, J. Saussey, J.-C. Lavalley, *J. Mol. Struct.* **1992**, *267*, 315 – 329.
[27] R. Matsuda, R. Kitaura, S. Kitagawa, Y. Kubota, R. V. Belosludov, T. C. Kobayashi, H. Sakamoto, T. Chiba, M. Takata, Y. Kawazoe, Y. Mita, *Nature* **2005**, *436*, 238 – 241.
[28] M. Fischer, F. Hoffmann, M. Fröba, *ChemPhysChem* **2010**, *11*, 2220 – 2229.
[29] R. Krishna, *RSC Adv.* **2015**, *5*, 52269 – 52295.
[30] P. Li, Y. He, Y. Zhao, L. Weng, H. Wang, R. Krishna, H. Wu, W. Zhou, M. O'Keeffe, Y. Han, B. Chen, *Angew. Chem. Int. Ed.* **2015**, *54*, 574 – 577; *Angew. Chem.* **2015**, *127*, 584 – 587.
[31] X. Duan, Q. Zhang, J. Cai, Y. Yang, Y. Cui, Y. He, C. Wu, R. Krishna, B. Chen, G. Qian, *J. Mater. Chem. A* **2014**, *2*, 2628 – 2633.
[32] J. Duan, W. Jin, R. Krishna, *Inorg. Chem.* **2015**, *54*, 4279 – 4284.

Received: July 23, 2015
Published online on October 30, 2015

CHEMISTRY
A European Journal

Supporting Information

Adsorptive Separation of Acetylene from Light Hydrocarbons by Mesoporous Iron Trimesate MIL-100(Fe)

Ji Woong Yoon,[a, b] Ji Sun Lee,[a, c] Sukyung Lee,[a] Kyoung Ho Cho,[a] Young Kyu Hwang,[a] Marco Daturi,[b] Chul-Ho Jun,[c] Rajamani Krishna,*[d] and Jong-San Chang*[a, e]

chem_201502893_sm_miscellaneous_information.pdf

Supporting Information (SI):

Fitting of pure component isotherms

The experimentally measured loadings for C_2H_2, and C_2H_4 in MIL-100(Fe) at temperatures of 293 K, and 313 K were fitted with the dual-site Langmuir model

$$q = q_{A,sat}\frac{b_A p}{1+b_A p} + q_{B,sat}\frac{b_B p}{1+b_B p} \quad (1)$$

with *T*-dependent parameters

$$b_A = b_{A0}\exp\left(\frac{E_A}{RT}\right); \quad b_B = b_{B0}\exp\left(\frac{E_B}{RT}\right) \quad (2)$$

The dual-site Langmuir model is required because the adsorption of C_2H_2, and C_2H_4 at the unsaturated metal sites is particularly strong.

The experimentally measured loadings for C_2H_6, and CH_4 in MIL-101(Fe) at temperatures of 293 K, and 313 K were fitted with the single-site Langmuir model

$$q = q_{A,sat}\frac{b_A p}{1+b_A p}$$

with *T*-dependent parameter

$$b_A = b_{A0}\exp\left(\frac{E_A}{RT}\right)$$

For all four guest molecules, both the adsorption and desorption branches of the component isotherms were fitted.

The fitted parameter values for C_2H_2, C_2H_4, C_2H_6, and CH_4 are provided in Table S1 (for activation at 423 K), and Table S2 (for activation at 523 K).

As illustration of the goodness of the fits, Figure 1 (Main manuscript) presents a comparison of absolute component loadings for C_2H_2, C_2H_4, C_2H_6, and CH_4 at 293 K, and 313 K in MIL-100(Fe) with the isotherm fits. The fits are excellent for all guest molecules over the entire pressure range at both temperatures.

Isosteric heat of adsorption

The binding energies of C_2H_2, C_2H_4, C_2H_6, and CH_4 in MIL-100(Fe) are reflected in the isosteric heat of adsorption, Q_{st}, defined as

$$Q_{st} = RT^2 \left(\frac{\partial \ln p}{\partial T} \right)_q \quad (3)$$

These values were determined by analytic differentiation of the pure component isotherm fits. For the dual-site Langmuir fits, explicit analytic expression for the Q_{st} is provided in the Supporting Information accompanying the paper by Mason et al.[1]; this procedure was followed in this work. Figure 2 of the main manuscript presents the calculated data on the loading dependence of Q_{st} for C_2H_2, C_2H_4, C_2H_6, and CH_4 in MIL-100(Fe). The values of Q_{st} follow the hierarchy $C_2H_2 > C_2H_4 > C_2H_6 > CH_4$; see Figure 2 (of main manuscript for heat of adsorption data, for activation at 423 K). The loading dependence of Q_{st} for C_2H_2, and C_2H_4 shows inflection characteristics. The initial high values reflect the strong binding of C_2H_2, and C_2H_4 with the unsaturated metal sites. Once all the metal sites are completely occupied, the Q_{st} reach plateau values. The binding of C_2H_6 and CH_4 in MIL-100(Fe) is considerably weaker, and no inflection characteristics are observed.

IAST calculations of adsorption selectivities

The data on the pure component isotherms, along with the isosteric heats of adsorption indicate that it is possible to separate mixtures of light hydrocarbons containing C_2H_2, C_2H_4, C_2H_6, and CH_4. In order to establish the feasibility of this separation we performed using the Ideal Adsorbed Solution Theory (IAST) of Myers and Prausnitz.[2]

Figure S1 presents IAST calculations of the component loadings for C_2H_2, C_2H_4, C_2H_6, and CH_4 for adsorption of a 4-component equimolar mixture in MIL-100(Fe) at 293 K, and 313 K. The IAST calculations show the following loading hierarchies at 100 kPa: $C_2H_2 > C_2H_4 > C_2H_6 > CH_4$. This hierarchy is the same as the hierarchy of binding energies, i.e. Q_{st} values.

On the basis of the component loadings, we calculate the selectivities of separation, S_{ads}, of the three constituent binary pairs: C_2H_2/C_2H_4, C_2H_4/C_2H_6, and C_2H_6/CH_4; see Figure 3a, and 3b (of the main manuscript). Each of the three selectivities are higher than about 2; this indicates that each of the four components can be recovered in nearly pure form from 4-component mixtures. In order to confirm this, we performed transient breakthrough simulations.

Simulations for transient breakthrough in fixed bed adsorbers

Fixed bed, packed with crystals of nanoporous materials, are commonly used for separation of mixtures such adsorbers are commonly operated in a transient mode, and the compositions

of the gas phase, and within the crystals, vary with position and time. For a given separation task, transient breakthroughs provide more a realistic evaluation of the efficacy of a material, as they reflect the combined influence of adsorption selectivity, and adsorption capacity.[3] To demonstrate the separation potential of MIL-100(Fe), we carried out transient breakthrough simulations using the methodology described in earlier work.[3, 4]

The simulation results for transient breakthrough are presented in terms of a *dimensionless* time, τ, defined by dividing the actual time, *t*, by the characteristic time, $\frac{L\varepsilon}{u}$. For the transient breakthrough simulations presented in this article, the following parameter values were used: mass of adsorbent = 0.5 g; inside diameter of tube = 4.15 mm, length of packed adsorber bed, *L* = 0.08 m; fractional voidage of packed bed, ε = 0.25; superficial gas velocity at inlet to the adsorber, *u*= 0.023 m/s. The mass of adsorbent = 0.5 g. In these simulations intra-crystalline diffusion resistances are considered to be of negligible importance.

Figure 8 of the main manuscript presents transient breakthrough simulation results for equimolar $C_2H_2/C_2H_4/C_2H_6/CH_4$/Ar mixtures at 313 K. The partial pressures of each hydrocarbon component in the entering gas mixture is 2.5 kPa. These simulations demonstrate that clean separations of each of the individual components. Video animations of the breakthrough are also uploaded as Supporting Information.

As validation of our breakthrough simulation methodology, Figure S6 presents a comparison of transient breakthrough simulations for equimolar $C_2H_2//C_2H_6$/Ar mixtures at 313 K, with experimental data under the same set of conditions using MIL-100(Fe) that is activated at 423 K. There is excellent agreement between the simulations and experiments. This agreement also demonstrates that intra-crystalline diffusion resistances are not important for C2 separations using MIL-100(Fe).

C_2H_2/CO_2 separations

Let us examine the potential of MIL-100(Fe) for C_2H_2/CO_2 mixture separations. This separation is important in industry for production of pure C_2H_2, that is required for a variety of applications in the petrochemical and electronic industries.[5] This separation is difficult because of the similarity in the molecular dimensions, and molecular properties.[3, 5, 6]

The experimentally measured isotherm for CO_2 at temperatures of 303 K was fitted with the single-site Langmuir model

$$q = q_{A,sat} \frac{b_A p}{1 + b_A p}$$

The Langmuir parameters are listed in Table S3. The isotherm data for C_2H_2 used in the selectivity calculations are for MIL-100(Fe) that is activated at 423 K.

Figure 9 of the main manuscript compares the IAST calculations of adsorption selectivity, S_{ads}, for separation of 50/50 C_2H_2/CO_2 mixtures for MIL-100(Fe) at 303 K with that of four other MOFs that also selectively adsorb C_2H_2: HOF-3,[7] CuBTC ,[7] ZJU-60a,[8] and PCP-33.[9] The IAST selectivity calculations for the four MOFs, available at 296 K, is taken from published work.[3]

We note that the selectivity using MIL-100(Fe) is higher than that of CuBTC, ZJU-60a, and PCP-33, but lower than that of HOF-3.

Transient breakthrough of C_2H_2/CO_2 mixture separations in Figure S7 demonstrates the separation potential of MIL-100(Fe).

Notation

b	Langmuir constant, Pa^{-1}
E	Energy of adsorption, J mol^{-1}
L	length of packed bed adsorber, m
p_i	partial pressure of species i in mixture, Pa
p_t	total system pressure, Pa
q_i	component molar loading of species i, mol kg^{-1}
q_t	total molar loading in mixture, mol kg^{-1}
q_{sat}	saturation loading, mol kg^{-1}
R	gas constant, 8.314 J mol^{-1} K^{-1}
t	time, s
T	absolute temperature, K
u	superficial gas velocity in packed bed, m s^{-1}
z	distance along the adsorber, m

Greek letters

	voidage of packed bed, dimensionless
	framework density, kg m^{-3}

Subscripts

i	referring to component i
t	referring to total mixture

Reference

[1] J. A. Mason, K. Sumida, Z. R. Herm, R. Krishna, J. R. Long, *Energy Environ. Sci*. **2011**, *4*, 3030-3040.

[2] A. L. Myers, J. M. Prausnitz, *A.I.Ch.E. J*. **1965**, *11*, 121-130.

[3] R. Krishna, *RSC Adv*. **2015**, *5*, 52269-52295.

[4] R. Krishna, *Micro. Mesop. Mater*. **2014**, *185*, 30-50.

[5] R. Matsuda, R. Kitaura, S. Kitagawa, Y. Kubota, R. V. Belosludov, T. C. Kovayashi, H. Sakamoto, T. Chiba, M. Takata, Y. Kawazoe, Y. Mita, *Nature* **2005**, *436*, 238-241.

[6] M. Fischer, F. Hoffmann, M. Fröba, *ChemPhysChem* **2010**, *11*, 2220-2229.

[7] P. Li, Y. He, Y. Zhao, L. Weng, H. Wang, R. Krishna, H. Wu, W. Zhou, M. O'Keeffe, Y. Han, B. Chen, *Angew. Chem. Int. Ed.* **2015**, *54*, 574-577.

[8] X. Duan, Q. Zhang, J. Cai, Y. Yang, Y. Cui, Y. He, C. Wu, R. Krishna, B. Chen, G. Qian, *J. Mater. Chem. A* **2014**, *2*, 2628-2633.

[9] J. Duan, W. Jin, R. Krishna, *Inorg. Chem*. **2015**, *54*, 4279-4284.

Table S1. Dual-Langmuir parameter fits for MIL-100(Fe). These parameters are for activation at 423 K.

	Site A			Site B		
	$q_{A,sat}$ mol kg^{-1}	b_{A0} Pa^{-1}	E_A kJ mol^{-1}	$q_{B,sat}$ mol kg^{-1}	b_{B0} Pa^{-1}	E_B kJ mol^{-1}
C_2H_2	1.4	1.39×10^{-15}	67	8.7	5.58×10^{-12}	34
C_2H_4	0.5	4.24×10^{-15}	64.2	8.8	2.12×10^{-11}	30
C_2H_6	33	1.55×10^{-11}	27.2			
CH_4	50	1.79×10^{-10}	15.2			

Table S2. Dual-Langmuir parameter fits for MIL-100(Fe). These parameters are for activation at 523 K.

	Site A			Site B		
	$q_{A,sat}$ mol kg^{-1}	b_{A0} Pa^{-1}	E_A kJ mol^{-1}	$q_{B,sat}$ mol kg^{-1}	b_{B0} Pa^{-1}	E_B kJ mol^{-1}
C_2H_2	1.6	1.45×10^{-8}	31.7	7	2.38×10^{-10}	26
C_2H_4	1.2	3.9×10^{-9}	35.7	5.5	5.34×10^{-11}	30
C_2H_6	18.3	7.36×10^{-12}	31.3			
CH_4	50	6.93×10^{-11}	18			

Table S3. Langmuir parameter fit for CO_2 isotherms in MIL-100(Fe) at 303 K.

	$q_{A,sat}$ mol kg^{-1}	b_A Pa^{-1}
CO_2	3.6	1.05×10^{-5}

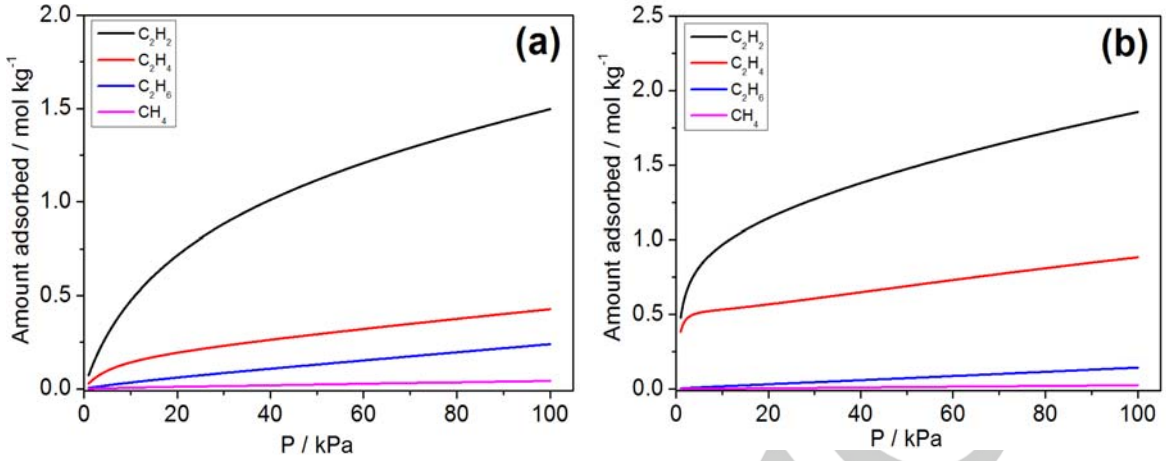

Figure S1. IAST calculations of the component loadings for C_2H_2, C_2H_4, C_2H_6, and CH_4 for adsorption of equimolar 4-component mixtures in MIL-100(Fe) at 313K. The sample was activated for 12 h at (a) 423 K and (b) 523 K.

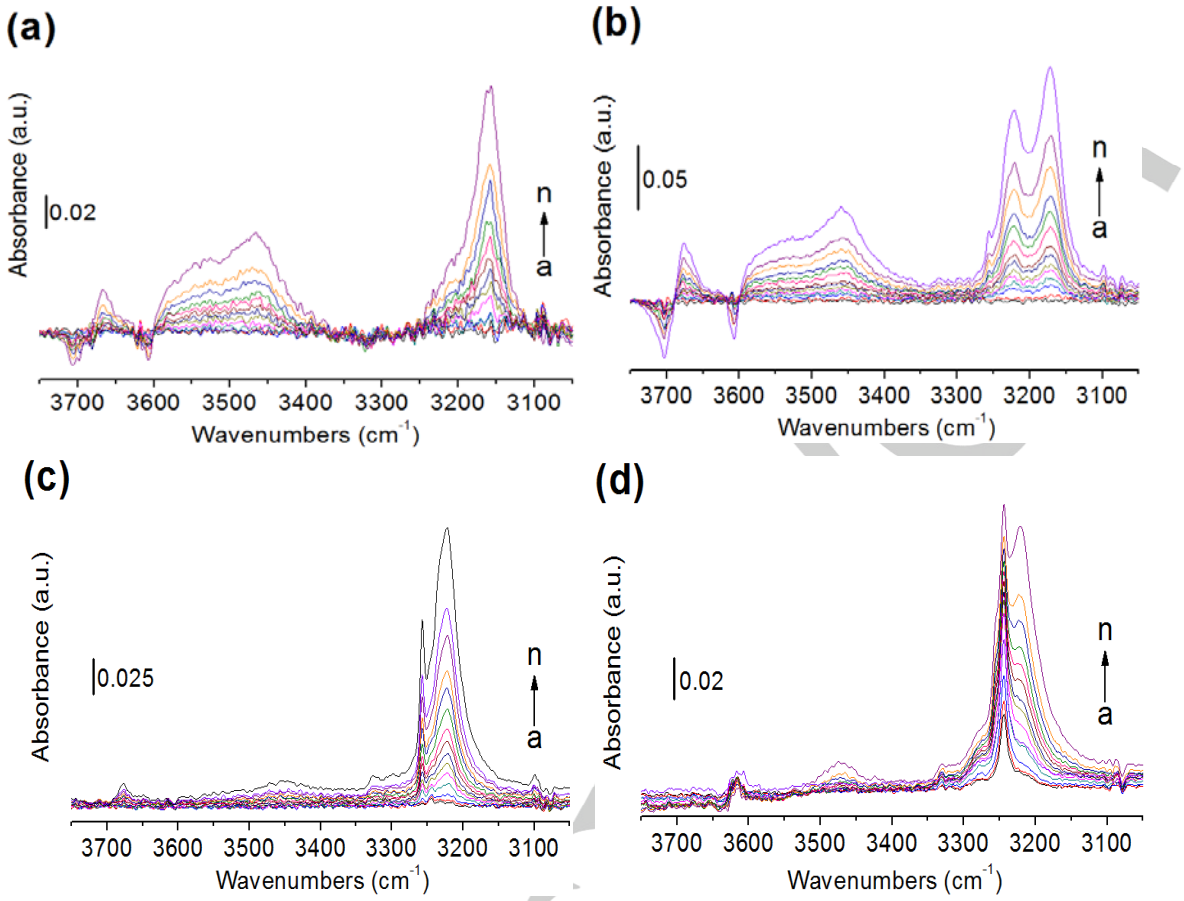

Figure S2. FT-IR spectra of acetylene adsorbed at 313 K on MIL-100(Fe) with increasing equilibrium acetylene pressures: (a) 10 ppm, (b) 20 ppm, (c) 40 ppm, (d) 80 ppm, (e) 160 ppm, (f) 240 ppm, (g) 300 ppm, (h) 400 ppm, (i) 500 ppm, (j) 600 ppm, (k) 800 ppm, (l) 1000 ppm, (m) 1200 ppm, and (n) 1500 ppm.

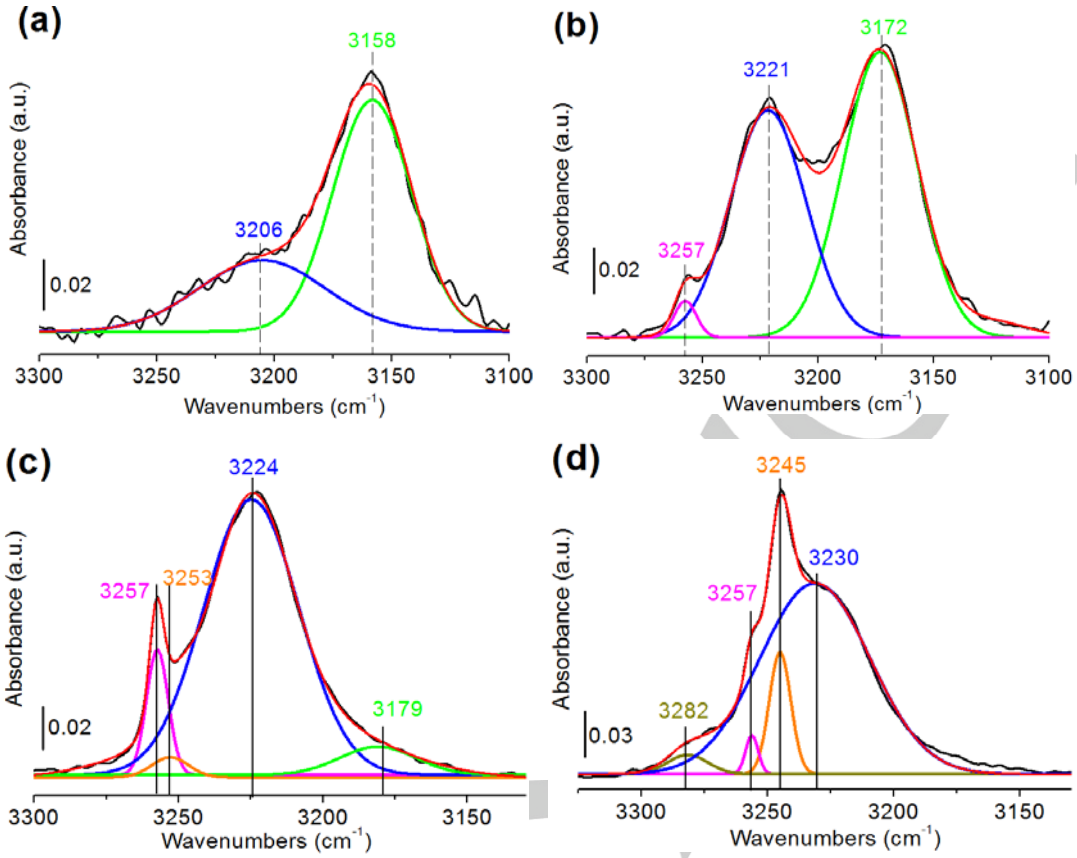

Figure S3. Deconvolution of the FTIR spectra of acetylene (1000 ppm) adsorbed on MIL-100(Fe) at 313 K after activation for 12 h under an argon flux at (a) 373 K, (b) 425 K, (c) 473 K, and (d) 523 K.

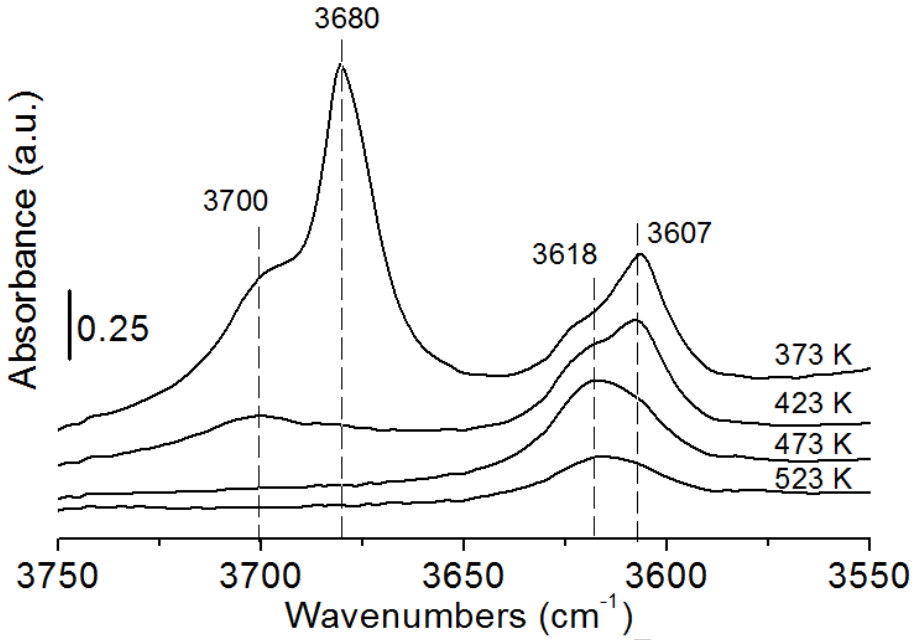

Figure S4. FT-IR spectra of MIL-100(Fe) activated at a range of temperature between 373 K and 523 K for 12 h under a flow of argon.

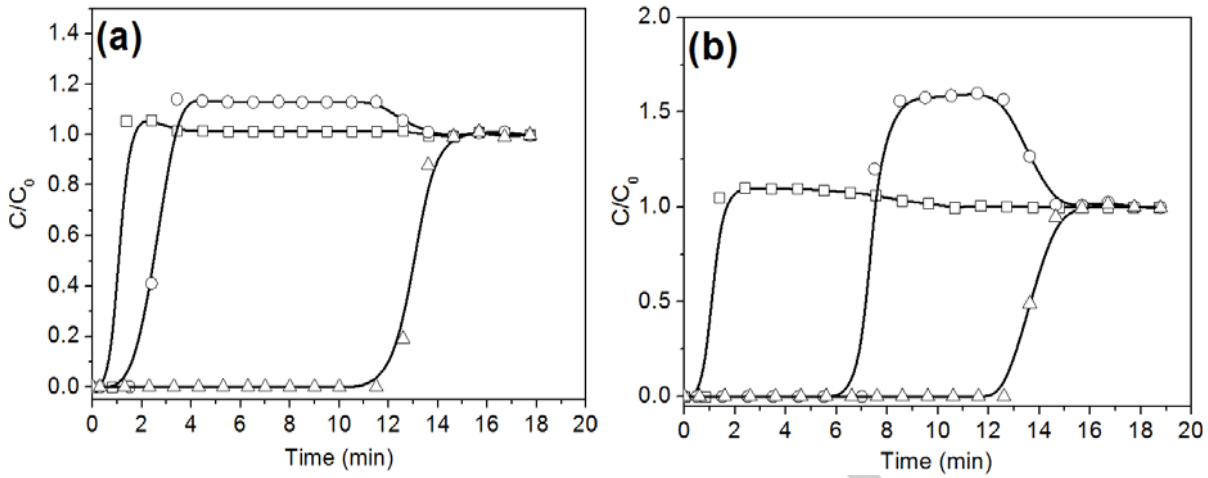

Figure S5. Breakthrough curves in the separation of an equimolar mixture of C_2H_6 (□), C_2H_4 (○), and C_2H_2 (△) in argon (p = 7.5 kPa) on MIL-100(Fe) at 313 K. The sample was activated for 12 h at (a) 423 K and (b) 523 K.

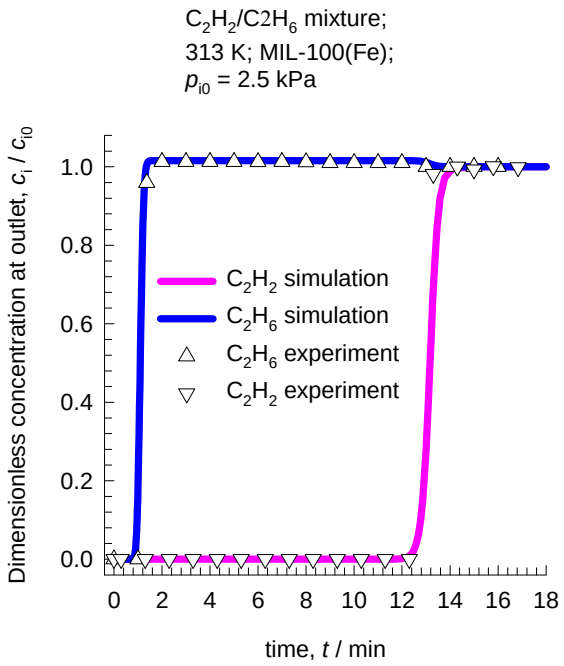

Figure S6. Transient breakthrough simulations for equimolar C_2H_2/C_2H_6/Ar mixture at 313 K on MIL-100(Fe) activated at 423 K for 12 h. The partial pressures of each hydrocarbon in the entering gas mixture is 2.5 kPa. The total pressure is 101 kPa. The symbols represent experimental breakthrough data for the same set of conditions.

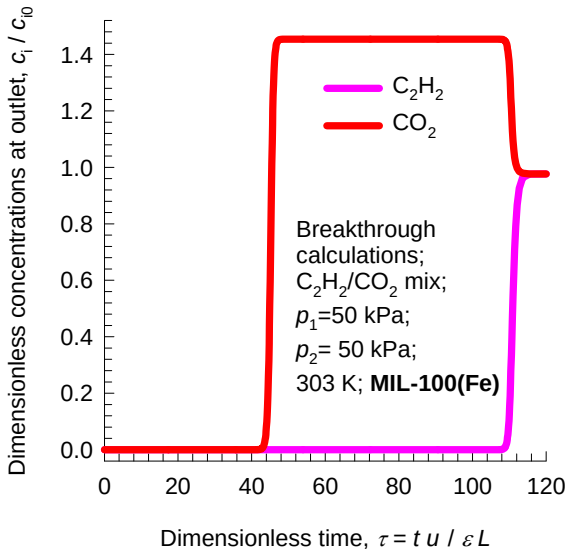

Figure S7. Transient breakthrough of C_2H_2/CO_2 mixture separations in a bed packed with MIL-100(Fe) at 303 K on MIL-100(Fe) activated at 423 K for 12 h.